

A Double Charge Density Wave in the Single Tellurium Square Net in $\text{Cu}_{0.63}\text{EuTe}_2$?

Christos D. Malliakas and Mercouri G. Kanatzidis*

Department of Chemistry, Northwestern University, Evanston, Illinois 60208

Received January 6, 2009; E-mail: m-kanatzidis@northwestern.edu

Interactions between electrons (charge or spin) and a distorted lattice may give rise to a variety of physical properties, such as superconductivity,¹ magnetoresistance,² ferroelectricity,³ charge density waves (CDWs),⁴ etc. A collective electron–phonon coupling in CDWs is thermodynamically favorable through a Peierls distortion. The understanding of electron instabilities, correlations, and electron–phonon interplay in matter is of fundamental importance. For example, manipulation of a CDW state by increasing the number of intercalated Cu atoms can lead to a superconducting state in Cu_xTiSe_2 .⁵

Polytelluride compounds with square nets of tellurium have been reexamined recently because of their ability to distort through CDWs.⁶ Orthorhombic RETe_3 (RE = rare-earth element) in particular has been recognized through angle-resolved photoemission spectroscopy (ARPES) as a model system for the study of Fermi-nesting-driven CDW distortions.⁷ The length and orientation of the CDW modulation vector in the polytellurides depend on the electronic structure and Fermi surface topology. A single incommensurate \mathbf{q} vector showing an anomalous behavior with temperature exists in most RETe_3 compounds.^{6,8} A common feature in RETe_3 is the presence of van der Waals gaps between the layers that contain the distorted Te nets. Prying the distorted Te nets apart, as manifested in the compounds AMRETe_4 ($A = \text{K, Na}$; $M = \text{Cu, Ag}$; $\text{RE} = \text{La, Ce}$) by intercalating neutral AMTe layers between RETe_3 layers, showed a unidirectional elongation of the CDW modulation vector.⁹ In tetragonal RETe_{2-x} where no van der Waals gaps exist and vacancies in the Te net are found, two symmetry-related orthogonal \mathbf{q} vectors are formed.¹⁰

Here we report a new type of CDW observed in the polytelluride compound $\text{Cu}_{0.63}\text{EuTe}_2$, which exhibits two superimposed, independent, and collinear incommensurate CDW vectors.¹¹ The expression of CDW in this fashion, where the distortion is dominated by two apparently independent waves propagating in the same direction, to the best of our knowledge has not been seen in any known CDW system. Density functional theory (DFT) calculations suggest a favorable Fermi-nesting distortion brought about by the stoichiometry of Cu.

The undistorted structure of $\text{Cu}_{0.63}\text{EuTe}_2$ ¹² adopts the space group $P4/nmm$ according to the CaMnBi_2 structure type (Figure 1A). It consists of Eu atoms surrounded by eight Te atoms in a square-antiprismatic geometry (Figure 1B). The Eu atoms are sandwiched between an anti-PbO-type layer of $[\text{CuTe}]^-$ and a square net of Te atoms (Figure 1C). The Cu site was found to be partially occupied with a refined fraction of 0.63(2). Although partial occupancy on this Cu site is unusual in the polytelluride family, it has been observed in the family of antimonides $M_x\text{LaSb}_2$ ($M = \text{Zn, Co, Mn, Cu}$; $x = 0.52\text{--}0.87$).¹³ The formula can be more expressly written as $[\text{M}_x\text{Te}]^{(2-x)-}\text{Eu}^{2+}[\text{Te}]^{x-}$, with an average electron count of 0.63(2) on the square-net Te atoms.¹⁴ The Eu–Te distances in the antiprism are 3.3193(6) Å and 3.4705(8) Å (Figure 1B), and the Te–Te distances in the square net are 3.1648(4) Å at 100 K (Figure 1C).

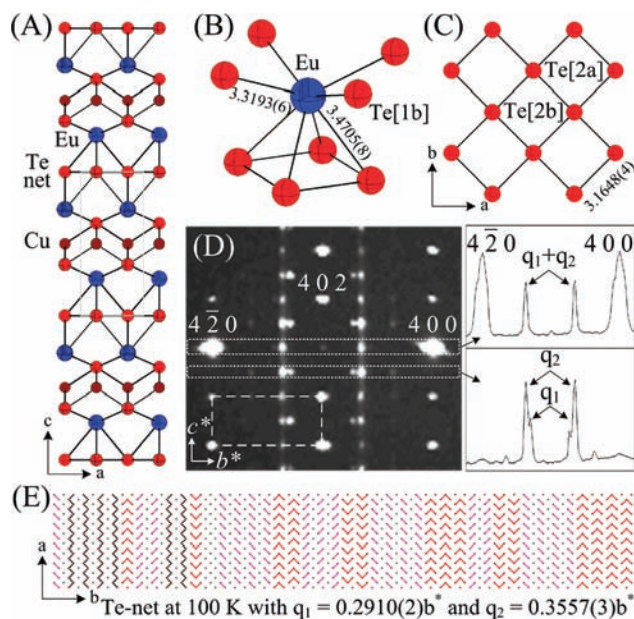


Figure 1. (A) Average structure of a $\text{Cu}_{0.63}\text{EuTe}_2$ subcell. (B) Coordination geometry of Eu in $\text{Cu}_{0.63}\text{EuTe}_2$. (C) Square net of Te atoms in the average structure of $\text{Cu}_{0.63}\text{EuTe}_2$. (D) Part of a synthetic precession photograph of the $(4kl)$ plane. A unit subcell is indicated with a dashed box. An intensity scan plot along the $4k0$ line (upper dotted box) shows the vector $\mathbf{q}_1 + \mathbf{q}_2$. An intensity scan along the $4k\frac{1}{2}$ line (lower dotted box) shows the two different vectors \mathbf{q}_1 and \mathbf{q}_2 . (E) CDW-distorted Te net in $\text{Cu}_{0.63(2)}\text{EuTe}_2$ at 100 K with $\mathbf{q}_1 = 0.2910(2)\mathbf{b}^* + \frac{1}{2}\mathbf{c}^*$, $\mathbf{q}_2 = 0.3557(3)\mathbf{b}^* + \frac{1}{2}\mathbf{c}^*$, and a bonding threshold of 3.118 Å.

Surprisingly, $\text{Cu}_{0.63}\text{EuTe}_2$ possesses two incommensurate modulation \mathbf{q} vectors, $\mathbf{q}_1 = 0.2910(2)\mathbf{b}^* + \frac{1}{2}\mathbf{c}^*$ and $\mathbf{q}_2 = 0.3557(3)\mathbf{b}^* + \frac{1}{2}\mathbf{c}^*$ (Figure 1D), and crystallizes in the $Pm(0\beta_1\frac{1}{2})(0\beta_2\frac{1}{2})0$ ($3 + 2$)-dimensional superspace group.¹¹ Temperature-dependent single-crystal X-ray diffraction showed that both \mathbf{q} vectors persist up to 500 K, which suggests a relatively wide energy gap.¹⁵ Their orientations remain unchanged, but their lengths increase with temperature. Specifically, the vectors are $\mathbf{q}_1 = 0.3051(3)\mathbf{b}^* + \frac{1}{2}\mathbf{c}^*$ and $\mathbf{q}_2 = 0.3471(4)\mathbf{b}^* + \frac{1}{2}\mathbf{c}^*$ at 300 K, $\mathbf{q}_1 = 0.3145(3)\mathbf{b}^* + \frac{1}{2}\mathbf{c}^*$ and $\mathbf{q}_2 = 0.3446(4)\mathbf{b}^* + \frac{1}{2}\mathbf{c}^*$ at 400 K, and $\mathbf{q}_1 = 0.3388(3)\mathbf{b}^* + \frac{1}{2}\mathbf{c}^*$ and $\mathbf{q}_2 = 0.3604(4)\mathbf{b}^* + \frac{1}{2}\mathbf{c}^*$ at 500 K.

The distortion is mainly located in the planar nets of Te (Figure 1C). The distribution of Te–Te distances has minimum, maximum, and average values of 2.922(5), 3.285(6), and 3.151(6) Å, respectively. The CDW in the Te net can be seen conveniently as a sequence of mainly trimers, dimers, and single Te atoms (Figure 1E). The minimum Te–Te distance in the zigzag chains is 3.070(5) Å and the maximum distance 3.116(5) Å. The zigzag chains are oriented perpendicular to the modulation direction. A similar type of atom interconnection found perpendicular to the modulation direction was observed for the RETe_3 family, but only very close

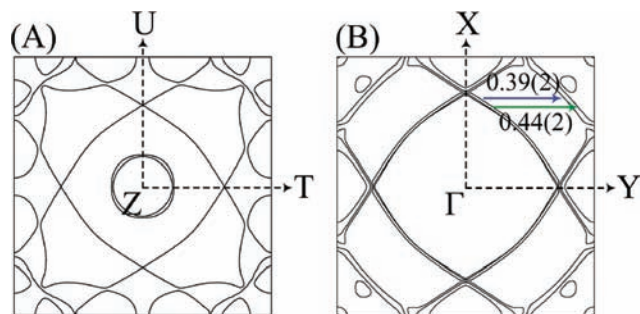


Figure 2. (A) Fermi surface topology for the average CuLuTe_2 structure (no CDW or vacancies). (B) Fermi surface topology for $\text{Cu}_{0.63}\text{LuTe}_2$. The two distinct nesting vectors along the Y direction are indicated.

to the CDW transition temperature.^{6b} In $\text{Cu}_{0.63}\text{EuTe}_2$, this interconnection between oligomers (monomers to form chains) in a direction normal to the modulation wave occurs at a low temperature (100 K) far from the CDW transition temperature (>500 K).

That $\text{Cu}_{0.63}\text{EuTe}_2$ has two CDW \mathbf{q} vectors pointing in the same direction despite the fact that it possesses only one type of Te net is very unusual. Canonically, only one such vector is expected.^{6–10} Multiple hybrid \mathbf{q} vectors have been observed in Sm_2Te_5 , but in that case, two separate and distinct Te nets with different electron counts exist.¹⁰ A possible weak, long-range ordering of Cu vacancies cannot be responsible for the appearance of the second \mathbf{q} vector in $\text{Cu}_{0.63}\text{EuTe}_2$. The modulated structure refines with no problems without the application of occupational waves on the Cu site, and the change in the residual intensities (electron density map) is negligible. The agreement factor based on all observed reflections (main and satellites) is essentially unchanged when ordering of Cu vacancies is assumed.

In order to understand the CDW distortions and the role of vacancies in the Cu layer, we performed calculations at the DFT level. The average structure of CuLuTe_2 (no CDW or vacancies) was used as a model. We observe that the bands around the Fermi level that have Te p-orbital character are more dispersed than those found in the layered RETe_3 polytellurides.¹⁶ This makes the Fermi surface more complex and very sensitive to small changes in the Fermi level.¹⁶ The calculated Fermi surface of CuLuTe_2 ($x = 1$) does not favor nesting of the bands since the topology does not have enough parallel regions in which nesting can occur (Figure 2A). However, this surface changes dramatically when Cu vacancies are present. In order to calculate more accurately the Fermi surface topology of the Cu-deficient structure, a threefold supercell ($1 \times 1 \times 3$) was created, and one Cu atom was removed from it to create the correct stoichiometry of “ $\text{Cu}_{0.67}\text{LuTe}_2$ ”. There are 24 bands that cross the Fermi surface. The Cu-deficient model reveals a very different overall Fermi surface topology, with two possible parallel nesting vectors with lengths of 0.39(2) and 0.44(2) (Figure 2B).¹⁷

The results of the calculations qualitatively account for the experimental observations and give some insight into the stability of the Cu-deficient compounds vis-à-vis the fully stoichiometric ones. It seems that it is necessary to remove electrons from the CuLuTe_2 system in order to have the Fermi energy level in a position where nesting is favorable, which can lead to the lower-energy CDW state. The system then accomplishes this required configuration by creating vacancies in the Cu plane.

In conclusion, $\text{Cu}_{0.63}\text{EuTe}_2$ possesses two observable superimposed, incommensurate, collinear modulation vectors, a feature that is unique among reported CDW materials. Theoretical considerations suggest the presence of a favorable Fermi-nesting-derived CDW distortion that is brought about by the presence of vacancies

on the Cu site. This discovery suggests that there are unanticipated nuances in the nature of the CDW state. It raises new questions about current understanding of CDW systems and how order emerges from electron correlations in the parent undistorted states. On the basis of the results reported here, examination of the structurally related but more complex quaternary AM_2EuTe_4 ¹² family is in progress in order to further probe the origin of this unique CDW behavior.

Acknowledgment. Support from the NSF (DMR-0801855, FRG-0703882) is gratefully acknowledged.

Supporting Information Available: Details of the structural analysis, results of the DFT calculations, and a CIF file. This material is available free of charge via the Internet at <http://pubs.acs.org>.

References

- Jorgensen, J. D.; Schuttler, H. B.; Hinks, D. G.; Capone, D. W.; Zhang, K.; Brodsky, M. B.; Scalapino, D. J. *Phys. Rev. Lett.* **1987**, *58*, 1024.
- Hwang, H. Y.; Cheong, S. W.; Radaelli, P. G.; Marezio, M.; Batlogg, B. *Phys. Rev. Lett.* **1995**, *75*, 914.
- Egami, T.; Ishihara, S.; Tachiki, M. *Science* **1993**, *261*, 5126.
- Grüner, G. *Density Waves in Solids*; Addison-Wesley: Reading, MA, 1994.
- Morosan, E.; Zandbergen, H. W.; Dennis, B. S.; Bos, J. W. G.; Onose, Y.; Klimczuk, T.; Ramirez, A. P.; Ong, N. P.; Cava, R. J. *Nat. Phys.* **2006**, *8*, 544.
- (a) Malliakas, C.; Billinge, S. J. L.; Kim, H. J.; Kanatzidis, M. G. *J. Am. Chem. Soc.* **2005**, *127*, 6510. (b) Malliakas, C. D.; Kanatzidis, M. G. *J. Am. Chem. Soc.* **2006**, *128*, 12612. (c) Kim, H. J.; Malliakas, C. D.; Tomic, A.; Tessmer, S. H.; Kanatzidis, M. G.; Billinge, S. J. L. *Phys. Rev. Lett.* **2006**, *96*, 226401.
- Schmitt, F.; Kirchmann, P. S.; Bovensiepen, U.; Moore, R. G.; Rettig, L.; Krenz, M.; Chu, J.-H.; Ru, N.; Perfetti, L.; Lu, D. H.; Wolf, M.; Fisher, I. R.; Shen, Z.-X. *Science* **2008**, *321*, 1649.
- A low-temperature-induced $\sim 1/3$ vector normal to the incommensurate one was reported for four RETe_3 compounds ($\text{RE} = \text{Dy, Ho, Er, Tm}$). See: Ru, N.; Condon, C. L.; Margulis, G. Y.; Shin, K. Y.; Laverock, J.; Dugdale, S. B.; Toney, M. F.; Fisher, I. R. *Phys. Rev. B* **2008**, *77*, 035114.
- (a) Malliakas, C. D.; Kanatzidis, M. G. *J. Am. Chem. Soc.* **2007**, *129*, 10675. (b) Patschke, R.; Kanatzidis, M. G. *Phys. Chem. Chem. Phys.* **2002**, *4*, 3266.
- Malliakas, C. D.; Iavarone, M.; Fedor, J.; Kanatzidis, M. G. *J. Am. Chem. Soc.* **2008**, *130*, 3311.
- Satellite reflections were found at six positions around the main reflections: $\mathbf{q}_1 = 0.2910(2)\mathbf{b}^* + 1/2\mathbf{c}^*$, $\mathbf{q}_2 = 0.3557(3)\mathbf{b}^* + 1/2\mathbf{c}^*$, $\mathbf{q}_3 = 0.3557(3)\mathbf{b}^*$, $\mathbf{q}_4 = 0.2910(2)\mathbf{a}^* + 1/2\mathbf{c}^*$, $\mathbf{q}_5 = 0.3557(3)\mathbf{a}^* + 1/2\mathbf{c}^*$, and $\mathbf{q}_6 = 0.3557(3)\mathbf{a}^*$. Vectors \mathbf{q}_4 , \mathbf{q}_5 , and \mathbf{q}_6 can be generated by 90° rotations of \mathbf{q}_1 , \mathbf{q}_2 , and \mathbf{q}_3 , respectively, around the c axis because of merohedral twinning. Only \mathbf{q}_1 and \mathbf{q}_2 are independent vectors, as \mathbf{q}_3 can be derived from \mathbf{q}_1 and \mathbf{q}_2 as follows: $\mathbf{q}_3 = 1 - (\mathbf{q}_1 + \mathbf{q}_2)$. In order to obtain a stable refinement and avoid nonlinear correlations between the rational and irrational components of the modulation vectors, a doubling of the cell along the c axis was performed to clear the rational part. Therefore, a centering vector of $(0\ 0\ 1/2\ 1/2)$ and a superspace group notation of $Xm(0\beta_10)(0\beta_20)0$ were used. As a result of this transformation, the two modulation vectors become collinear. A STOE IPDS II diffractometer was used to collect intensity data (Mo $K\alpha$ radiation). Direct methods in the SHELXTL software (Sheldrick, G. M. *SHELXL-97: Program for Crystal Structure Refinement*; University of Göttingen: Göttingen, Germany, 1997) were used to find the atomic positions in the subcell. An analytical absorption correction was performed, and the structure was refined with the JANA2006 software (Petricek, V.; Dusek, M.; Palatinus, L. *JANA2006*; Institute of Physics: Praha, Czech Republic, 2006). Crystallographic data for $\text{Cu}_{0.63}\text{EuTe}_2$: superspace group, $Xm(0\beta_10)(0\beta_20)0$; $\mathbf{q}_1 = 0.2910(2)\mathbf{b}^*$, $\mathbf{q}_2 = 0.3557(3)\mathbf{b}^*$; $Z = 4$; $a = 4.4536(2)$ Å, $b = 4.4723(2)$ Å, $c = 20.2982(8)$ Å; $V = 404.30(3)$ Å³; 17326 reflns collected (1621 main + 15705 satellite), 9210 unique reflns (947 main + 8263 satellite) ($R_{\text{int}} = 0.0576$); $R = 0.066$, $wR = 0.113$ for reflections having $I > 3\sigma(I)$; min/max residual electron density = $-3.46/3.83$ e Å⁻³.
- Patschke, R.; Brazis, P.; Kannewurf, C. R.; Kanatzidis, M. G. *Mater. Chem.* **1999**, *9*, 2293.
- Coldier, G.; Schafer, H.; Woll, P. Z. *Naturforsch.* **1985**, *40b*, 1097.
- When Eu is coordinated to a chalcogen atom, it usually adopts a 2+ valence. The energy of the f orbitals of Eu is lower than the energy of the p orbitals of the chalcogen (especially Se or Te), so Eu^{3+} always gets reduced to Eu^{2+} by the chalcogen atom.
- A partial gap opens at the Fermi level due to the CDW distortion. The system remains metallic, but increasing the gap raises the transition temperature of the CDW.
- More information can be found in the Supporting Information.
- We calculated the average value of 0.39(2) from the minimum value of ~ 0.37 for the nesting vector (close to the Y point) and the maximum of ~ 0.41 (close to the X point).

JA900091F